An Investigation into Spatial and Temporal Aspects of Transient Stability in Power Systems with Increasing Renewable Generation

Robert I. Hamilton [1*], Panagiotis N. Papadopoulos [1*], Keith Bell [1]

[1] Department of Electronic and Electrical Engineering, Institute for Energy and Environment, University of Strathclyde, 16 Richmond St, Glasgow, Scotland
[*]robert.hamilton@strath.ac.uk, panagiotis.papadopoulos@strath.ac.uk

Abstract: This paper investigates the impact of generator dispatch (dictated by cost) and locational aspects related to renewable generation connection and consequent disconnection of synchronous generation, on transient stability. As conventional synchronous generation (SG) is displaced by power electronic converter interfaced generation (PEC), the transient behaviour of the power system may change significantly due both to the changed power flows resulting from the different locations of renewables compared with thermal plant and the different dynamic characteristics of PEC. This paper uses an AC Optimal Power Flow (OPF) to determine credible, minimum cost dispatches of generation in a test network with increasing penetration of PEC in different locations. It is found that the critical locations of the system can vary significantly with respect to economic dispatch, location of disconnection of SG and location of PEC, highlighting the increasing temporal and spatial change in system dynamic behavior.

1. Introduction

The drive to decarbonise electrical power generation as well as other policy decisions (e.g. decisions to decommission nuclear power plants in some countries) has resulted in conventional synchronous generation (SG) such as coal and gas plant, being displaced by renewable generation interfaced by Power Electronic Converters (PEC), such as wind and solar resources [1, 2]. The low marginal cost should result in the power available from renewables being fully dispatched, provided the system's operating limits can accommodate it. In addition to causing changes in the operating point and number of connected generators in operational time, in the long-run this also results in a reduction in the number of SGs connected to the power system due to decommissioning of conventional generating units (e.g. coal or nuclear power plants). This has an impact on operability of the power system, in particular its dynamics, especially transient stability [3].

The response of SGs is governed by the nonlinear power-angle relationship and is influenced by numerous factors including the generator's inertia, loading, internal voltage magnitude and internal reactance, fault clearing time and fault location [4]. As SG is increasingly displaced by PEC (such as type III and IV wind turbines), a number of these factors are affected which has a knock-on impact on the transient stability. The fact that many of these parameters change at the same time when PECs are connected to existing networks, makes identifying their impact on system stability a difficult and complicated task. Additionally, the difference in the physical characteristics of SG and PEC means that their interaction with the grid is significantly different, rendering the aforementioned task even more complicated. The rotating parts of a SG are electromagnetically coupled to the power system, meaning that they inherently provide synchronising torque and inertia to the system. This is not the case for PEC, where the power electronic interface decouples the rotational mass (if any) from the grid [4]. As SG is displaced by PEC, the inertia of the system reduces meaning that the natural reaction of the system to a disturbance speeds up [5]. Some converter-interfaced technologies possess fault ride through (FRT) capabilities, enabling them to ride through faults in order to enhance system stability (through a rapid reduction in active power output and injection of reactive power) [6, 7].

Numerous studies suggest that as SG is displaced by PEC, there is a significant impact on angular stability in power systems. It can be hard to predict to what extent different parameters influence the stability boundary – be it an improvement or deterioration [5, 8] – due to the complexity of the nonlinear dynamic behaviour of power systems. The uncertain nature of renewable generation means that the pre-disturbance operating conditions and the number of connected SGs tend to vary more, reshaping the stability boundary in operational time [9]. For example the authors in [10] find that the volume of PEC connected is an important factor in determining the angular stability of the network. Qi et al find that the influence of uncertainties in PEC become influential when penetration exceeds 30% [11]. Authors in [12] cite 'non complimentary characteristics' between SG and PEC as a reason for deteriorations in stability where there is a mix of generator technologies in a particular region (rather than a high penetration of either). [13] goes further, proposing a voltage sensitivity based index to identify network locations where the connection of PEC would have a beneficial and detrimental impact on angular stability. [14] demonstrates how the SG that is displaced and the fault location are crucial in shaping the stability boundary. Locational aspects are further considered in [15], where it is found that 'symmetrical' displacement of SG by PEC (i.e. evenly distributed throughout the network) has a beneficial impact on transient stability. Fault location with respect to PEC location is considered in [16], where angular stability is found to either improve or deteriorate based on the proximity of the fault to PEC. However no effort is made to quantify what is meant by 'near' or 'far'. Findings are supported by [17], where it is concluded that stability depends on the relative position of the PEC (in this case energy storage) with respect to both the fault and SG. Post-fault active power recovery rate of PEC is also found to have a significant impact on the stability boundary in [18], depending on

whether PEC is located in an exporting or importing network area. This is further analysed in more general terms in [19]. Other parameters found in literature to impact the angular stability boundary include level of system inertia and synchronising torque [20].

In addition to locational aspects presented above, the link between generator cost and dispatch (i.e. loading) is well-known and is based on fundamental economic principals. Moreover, it is widely acknowledged that the loading of SG will have a significant impact on its susceptibility to losing synchronism following a transient event [4]. There is therefore a link between generator cost and transient stability, motivating studies whereby transient stability is included as a constraint in the OPF. For example, [21] highlights the conflict between transient stability and the economic objective and propose a risk-averse multi-objective generation dispatch model to balance this. In [22], transient stability is included in the economic dispatch problem, minimising risk of transient instability.

However, to the extent of our knowledge, the combined impact on transient stability of economic dispatch as well as location of PEC in the context of power systems with increasing penetrations of PEC has not yet been systematically identified using detailed RMS models and time domain simulations, so further work is needed. Moreover parameterisation of locational aspects is missing in current literature, and so is addressed by this paper.

This paper presents initial results considering the impact on first swing rotor angle stability (referred to as angular stability hereinafter) from displacement of SG (with different costs) by PEC in different network locations (i.e. disconnection in high vs. low cost areas). An AC Optimal Power Flow (OPF) is used to determine the dispatch of generators on a three-area test network. These initial studies aim at identifying patterns arising from the combined impact of varying fault location, volume and location of SG, PEC penetration and PEC location on angular stability within the context of economic dispatch. Furthermore, locational parameters relating to changes in angular stability are quantified using the network admittance matrix, the electrical distance ratio (EDR - a relevant metric defined in this paper to capture the combined effect of SG disconnection and the electrical distance between a SG and a PEC unit) and short-circuit capacity. Special attention is given to the identification of cases when there is a change in critical area (i.e. area with the lowest CCT and consequent switch in the most critical SG) due to the aforementioned variation of parameters related to generator cost and locational aspects under increasing penetrations of PEC.

Whilst results presented may be network specific, this paper presents a systematic way to investigate the impact of generator cost and locational aspects related to PEC on the transient stability of a power system. What is more, the methodology developed and metrics used are unique and can be applied to any network to extract results and draw conclusions.

2. Methodology

Studies are performed using a simple but detailed RMS power system model primarily in order to identify key parameters that impact angular stability in power systems with increasing penetrations of PEC in different areas (high vs. low cost) of the network. The dispatch of generation is determined by an AC OPF with simple linear cost curves (with high, medium or low incremental cost) that are swapped between the machines systematically to determine different generator dispatches (effectively changing the merit order), which in turn will likely impact angular stability. The impact on the stability boundary of generator cost is discussed in Section 3.1, locational aspects in Section 3.2 and the sensitivity of SGs to changes in active power output in Section 3.3. An overview of the methodology is outlined in Fig. 1 and the remainder of this section details the methodology used to obtain results.

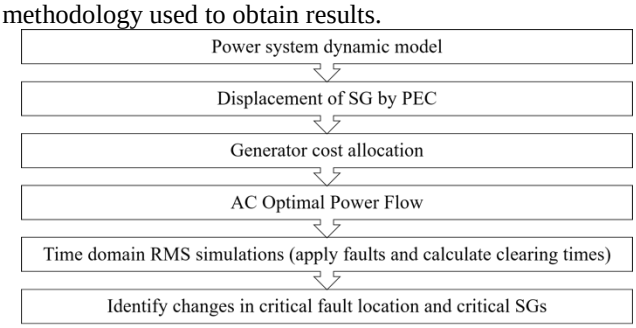

Fig. 1. *Procedure used to generate credible operational scenarios and assess network stability.*

2.1. Power System Dynamic Model

This paper uses a modified version of the Anderson-Fouad 9 bus model (Fig. 2) implemented in DIgSILENT PowerFactory [23]. The network nominal voltage is 230 kV, and the nominal frequency is 60 Hz. The total active power demand of the network is 315 MW, modelled as balanced three-phase constant impedance loads in the dynamic simulation.

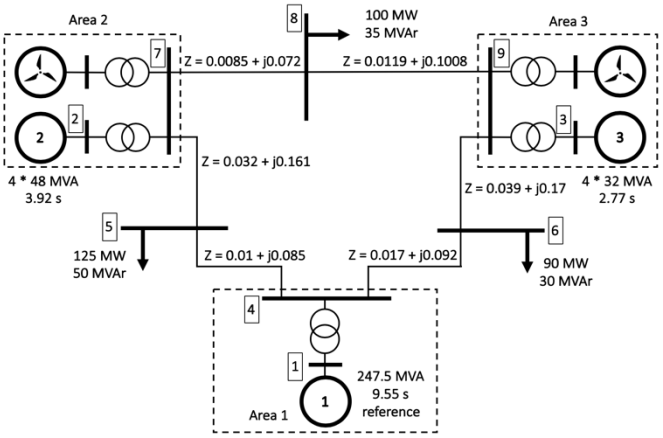

Fig. 2. *Anderson-Fouad 9-Bus model adapted to include IEC Type 4A wind turbines in different areas.*

There are three SGs in the network, represented by full detail four winding models (6^{th}-order). SG_2 and SG_3 are assumed to represent four equal-sized units (to simplify SG displacement in Section 2.2). Additional details regarding the parameters of the network and machines can be found in [23]. The reference machine is SG_1 which is rated at 247.5 MVA with an inertia constant of 9.55 seconds. SG_2 is a 192 MVA machine with an inertia constant of 3.92 seconds (representing four 48 MVA machines), equipped with an IEEE DC1C automatic voltage regulator (AVR) and a power system stabiliser (PSS). SG_3 is the smallest machine on the network at 128 MVA with an inertia constant of 2.77 seconds

(representing four 32 MVA machines). All generators have an operating region from 0.35 to 1 p.u. active power loading and -0.25 to 0.5 p.u. reactive power loading. No protection devices are modelled.

International Electrotechnical Commission (IEC) type 4A wind turbines [24] are used to model wind generation in these studies. Using the assumption that PEC is not required by grid code to provide voltage control, the controller operates at unity power factor i.e. no MVArs are injected into the system [25]. It should be noted that this capability may vary from system to system and will impact reactive power dispatch and therefore transient stability. However, the investigation of this capability remains out of the scope of this paper and is left for future work, focusing more on active power dispatch changes due to different generator costs. The wind turbines used have FRT capability and reactive power support. Reactive power injection is controlled as the pre-fault value plus an additional voltage dependent reactive current injection during the fault, and as the pre-fault value plus an additional constant reactive current injection post-fault. A windfarm is treated as an aggregate of individual 1 MW turbines, each with its own transformer, where the total output of the windfarm is the summation of each individual turbine's active power output. The volume of wind and its location on the network depends on the particular displacement scenario, defined in Section 2.2 below.

To simplify analysis of the network, three generating areas have been defined and will be referred to as areas 1, 2 and 3 throughout this paper. The three load busses are not part of any area in particular so will be referred to by their bus number.

2.2. Conventional SG Displacement by PEC

To simplify the studies PEC connecting in one area of the network will displace the SG in the same area, and displacement will only occur in one area at a time. No displacement in area 1 is studied, because SG_1 is the reference machine with the largest rating and inertia and is therefore a very stable machine. As a starting point when defining the scenarios explained in detail below, the volume of PEC connecting in area 2 and 3 is based on the active power export from each area from the original load flow solution, with no wind generation (Table 1).

Table 1 Active power dispatch from original load flow solution [23]

Network Area	1	2	3
Original Load Flow (MW)	71.6	163.0	85.0

Table 2 Displacement cases used in studies showing SG machine rating and volume of wind generation

Case	Displacement Case	Area 1	Area 2		Area 3	
		SG_1 MVA	SG_2 MVA	PEC_2 MW	SG_3 MVA	PEC_3 MW
Base	0%	247.5	192.0	0.0	128.0	0.0
1	25% A2	247.5	144.0	40.0	128.0	0.0
2	50% A2	247.5	96.0	81.0	128.0	0.0
3	75% A2	247.5	48.0	122.0	128.0	0.0
4	25% A3	247.5	192.0	0.0	96.0	21.0
5	50% A3	247.5	192.0	0.0	64.0	42.0
6	75% A3	247.5	192.0	0.0	32.0	63.0

The seven displacement scenarios are defined by a displacement percentage and displacement area and outlined in Table 2. For example; case 1 illustrates 25% displacement of SG by wind in area 2. This means 25% penetration of wind generation from the original load flow solution (25% of 163 MW, equating to 40 MW when rounded down to the nearest MW) and the disconnection of 25% of SG_2 (one of the four 48 MVA units which it represents, leaving three units connected with a combined rating of 144 MVA). The active and reactive power operating points of all SGs are obtained from the OPF solution. The base case has no displacement in any area.

2.3. Fault Clearing Time, Stability Indicies and Criteria for Instability

In angular stability studies, critical clearing time (CCT) is frequently used as an indicator of the severity of a fault. For transmission system faults, the main protection may generally be expected to operate within 100 ms [7], so a CCT that is approaching this threshold can be considered critical. Conversely, CCTs greater than 500 ms are considered to be non-critical in this paper. CCT is therefore used in this paper as a metric for transient stability.

Since the location of the fault with respect to each SG is important for transient stability, the CCT is determined at each busbar on the network for each displacement scenario and cost allocation. To do so, a balanced three-phase-to-ground fault is applied at each busbar on the network in turn, and the CCT is determined by iteratively increasing the fault duration. After the fault is cleared, the network returns to the pre-fault network topology with no generators or lines tripping, i.e. three-phase self-clearing faults. In order to do so, the criteria for instability must first be defined. In the relevant literature, the angle limit used for stability analysis varies [25]. This paper uses a heuristic limit on the rotor angle deviation for identifying transient instability. A SG losing synchronism will accelerate with respect to its initial synchronous rotation at nominal speed, which in turn will result in an advancement of the rotor angle from the initial steady-state angle [7]. If the difference between any two SG rotor angles is greater than π at an instance in time, then the system is considered unstable as outlined in (1) - since this would result in a "pole slip".

$$\Delta\delta_{ij} = \delta_i - \delta_j > \pi \quad (1)$$

where δ_i and δ_j are the rotor angles of SGs *i* and *j*. For example, if $\delta_i > \delta_j$ and SG_i has the greatest initial acceleration, then SG_i is the first SG to go unstable. It should be noted that all these angles refer to dynamically changing states during a time domain RMS simulation and are not related to the steady-state angles of the power flow solution.

In terms of defining changes in angular stability, the following stability indices are used to describe the stability boundary in this paper; the area of the network that contains the busbar with the shortest CCT (CCT_{min}) from a particular scenario is referred to as the critical fault location (CFL), and the generator that loses synchronism at the CFL is referred to as the critical SG (CSG). The CCT for a particular busbar fault may be abbreviated to $CCT_{bus\#}$ (for example; CCT_6 denotes the CCT at bus 6).

2.4. AC OPF and Allocation of Generator Costs

An AC OPF [26] is used to determine the dispatch of the SGs on the test network using the inbuilt AC OPF solver

in DIgSILENT PowerFactory. Whilst real market operations might lead to different generator dispatches in real operation, in this paper it is assumed that the OPF solution is a reasonable representation to generate credible generator dispatches. Each generator on the network is allocated either a high (H), medium (M) or low (L) incremental cost to establish a merit order between the SGs. Each incremental cost (H, M or L) is only ever allocated to one generator at a time meaning that there is a total of six cost combinations for the three SGs. As wind has no fuel cost [27], and thus no associated cost in the OPF, it will operate at 100% of rated power when connected to the network. The exact dispatch of generation is determined by the OPF, with the objective of minimising the total generation cost whilst respecting constraints (such as generator loading, bus voltages and line loadings). This results in PEC operating at full active power output, cheaper SG running at a high active power loading, and the more expensive SG running at lower active power loading.

Generator cost allocations are referred to using a three-letter code, with the first letter referring to the cost of SG_1, the second SG_2 and the third for SG_3. For example, a *'HML'* cost code means that SG_1 is most expensive, followed by SG_2 and SG_3 is the cheapest. The incremental costs for each cost allocation are given Table 3. Incremental costs here are designed only to determine a credible dispatch of generation (i.e. the cost of the dispatch is not important for these studies). As a generator is displaced (as outlined in Section 2.2), the operating range (i.e. the minimum and maximum absolute active power limits (which corresponds to an operating range of 30 - 85% of S_{rated})) of the SG will reduce, however, the incremental cost stays the same.

Table 3 Incremental cost of synchronous generators in each cost allocation (£/MW)

	HML	HLM	MHL	MLH	LHM	LMH
SG_1	1.47	1.47	0.73	0.73	0.07	0.07
SG_2	0.95	0.09	1.89	0.09	1.89	0.95
SG_3	0.14	1.42	0.14	2.84	1.42	2.84

The rationale behind the approach used in this paper of changing generator costs is to establish a wide range of possible operating scenarios that could be observed in different power systems. These systems may have different generation mixes in different locations due to variations in generator availability or changes in relative fuel costs or even in the same system due to decommissioning of certain types of generators potentially causing a change in the cost (i.e. not suggesting that generator costs will fluctuate like this in operational time frames). For example, the impact of a low-cost SG being displaced by PEC may result in different changes to the dynamic behaviour of the system than if a high or medium-cost SG is displaced.

2.5. Locational Aspects

To assess locational aspects; the pre-fault network admittance matrix (a measure of electrical distance between key network locations), electrical distance ratio (EDR, defined below) and short-circuit capacity from synchronous sources at different network locations (a measure of network strength) are used. Important locational aspects include fault location, SG location, PEC location and the location of displacement – all with respect to each other. Moreover, the location of the CSG with respect to the aforementioned aspects is likely to be important, since the CSG dictates CCT_{min} (for example, the location of the CSG with respect to PEC may be of interest).

2.5.1. Network Admittance Matrix: The base case network *9 by 9* pre-fault admittance matrix is formed following the process described in [23], with appropriate values of transient reactance (x_d') included. For cases 1-6, six separate *10 by 10* admittance matrices are formulated since varying volumes of PEC are connected in different areas of the network. PEC is connected to the network through transformers in parallel, resulting in an increased admittance between PEC and the point of connection with the grid as PEC penetration increases (and consequently number of connected wind turbines). Elements of the admittance matrix are identified as: $\overline{Y}_{ii}$ for the sum of admittances connected to bus *i*, and $\overline{Y}_{ij}$ for the negative of the admittance between bus *i* and *j*. Since this paper is interested in the location of power system components (connected at different busbars) with respect to each other, the electrical distance between said busbars is of interest (i.e. the non-diagonal elements of the admittance matrix).

2.5.2. Electrical Distance Ratio (EDR): The relationship between SG transient reactance (x_d'), the impedance between PEC and the network (impedance from PEC terminals to the high-voltage side of the grid transformer), and the overall network impedance is important – since the impact on the net electrical distance between SG and PEC is dependent on the magnitude of each parameter. These values can be derived from the network admittance matrix for different displacement scenarios. The electrical distance ratio (EDR) has been created for this paper and is defined as the ratio between the transient reactance of a SG (x_d'), and the electrical impedance from the terminals of that same SG to the terminals of PEC (denoted as x_{grid} in Equation 2, comprising of the impedance of the SG transformers ($x_{SG_{trnf}}$), PEC transformers ($x_{PEC_{trnf}}$) and network impedance between the generators ($x_{network}$).

$$EDR = \frac{x_d'}{x_{SG_{trnf}} + x_{PEC_{trnf}} + x_{network}} = \frac{x_d'}{x_{grid}} \quad (2)$$

The EDR accounts for the changes to electrical distance between SGs and PEC as a result of displacement, providing a metric that describes the proximity of PEC to SG on the network. This is done through a comparison of the effective electrical distance between the transient reactance of SG (i.e. how large or small the rating of the SG is) with respect to the electrical distance coming from the SG terminals to the PEC unit (including the network impedance).For example, an EDR below 1 indicates that the transient reactance of the SG is smaller than the impedance between the SG terminals and PEC, whilst a EDR above 1 indicates that the transient reactance is larger. As a result, it is useful in highlighting the extent to which FRT capability (related to reduction in active power output and increase in reactive power) from PEC can positively impact SG.

2.5.3. Short-Circuit Capacity: The short-circuit capacity is used here as a measure of system strength. Short-circuit calculations are performed according to IEC 60909 [28] in DIgSILENT PowerFactory for each displacement scenario,

with PEC disconnected from the network. The reason for this choice is to quantify only the effect of reducing synchronous generation, neglecting the dynamic behaviour of PECs in this metric, which is considered in detail in RMS time domain dynamic simulations performed, when calculating the CCTs. Therefore, this metric reduces with increasing penetrations of PEC and consequent disconnection of SGs.

2.6. Time Domain RMS Simulations

Time domain RMS simulations are performed for each displacement case (Table 2) with each of the six possible cost combinations (Section 2.4) resulting in 42 different scenarios and the stability indices along with all the above mentioned parameters are calculated. Since full IEC type IV wind dynamic models are used to model, the impact of the dynamics of wind – including the FRT capabilities – impact the dynamic response of the network.

3. Results

Three important factors that have a significant impact on the stability boundary are analysed in this section. The first is generator cost (i.e. active power loading) with no displacement of SG by PEC. The second is locational aspects that influence the stability boundary (interrogated through the network admittance matrix). Finally, the impact of SG sensitivity to changes in active power output (dependent upon generator incremental cost, SG MVA-rating, PEC penetration, and demand level). This section presents a number of case studies to highlight correlations between these factors and subsequent changes to the shape of the stability boundary. In general terms, it is found that:

- generator cost dictates the general shape of the stability boundary (low-cost SGs dispatched with high active power loading, resulting in shorter CCTs for nearby faults);
- locational aspects result in either improvements or deteriorations to the stability boundary, depending on the location of connection of PEC with respect to the CSG (near to versus far from) and;
- SGs with high sensitivity to changes in active power loading can also result in significant changes to the stability boundary in different displacement cases.

It is important to note that these factors cannot be considered in isolation, since they all ultimately affect the stability boundary. It is difficult to decouple the impact of any one parameter to determine the extent to which it impacts the stability boundary due to the complexity and nonlinearity of the problem. What is more, the extent to which each factor contributes to the shape of the stability boundary changes depending on the specific case. In certain cases, this can result in significant changes to the stability boundary such that the CCT_{min}, CFL and CSG can move around the network.

3.1. Impact of Generator Cost (Dictating Active Power Loading) and non-Operational Parameters

It is widely known that generator cost (i.e. active power loading of SG) will have a marked impact on angular stability, with highly priced generators operating far from the stability boundary, whilst cheaper generators operate much closer to it. In addition to this, non-operational parameters (such as SG MVA-rating and inertia) also play an important role. The objective of this section is to (a) illustrate how the marginal costs determine generator dispatch, (b) illustrate the extent of the impact that generator cost can have on angular stability and (c) highlight the impact that the aforementioned non-operational parameters on angular stability in the network used.

In Table 4, the base case for all cost allocations are compared (i.e. there is no displacement of SG by PEC, and since the size of each SG remains the same, total system inertia remains constant). The only parameter changed is the generator cost which primarily alters the active power dispatch of SGs. It should be noted that changes in reactive power flows also occur which can also affect system stability.

Table 4 CCT_{min}, CFL, CSG and % of maximum SG active power loading in the base case for all cost allocations

Cost Allocation	CCT_{min} (ms)	CFL (Busbar)	CSG	Active Power Loading (%)		
				SG_1	SG_2	SG_3
LMH	540	1	SG_1	100	43	35
LHM	420	3	SG_3	100	35	46
MLH	210	2	SG_2	56	100	35
HLM	210	2	SG_2	38	100	71
MHL	170	3	SG_3	72	35	100
HML	170	3	SG_3	35	83	100

The active power loading of SGs (Table 4), shows how each cost allocation establishes a clear merit order between SGs using the incremental costs outlined in Section 2.4 – resulting in the lower priced SGs having higher active power loading. Consequently, CCT_{min} varies significantly from a minimum 170 ms up to a maximum of 540 ms. More importantly, the CSG and CFL changes between different cost allocations – highlighting the significance of generator cost in the angular stability problem.

Apart from the impact of generator cost, the impact of SG non-operational parameters (i.e. MVA-rating and inertia) are also observed in Table 4. In general terms CCT_{min} can be seen to reduce with the MVA-rating and inertia of the generator with the low-cost, with the longest times when SG_1 (largest MVA-rating and inertia) is the low-cost generator and the shortest times when SG_3 (smallest MVA-rating and inertia) is the low-cost generator. What is more, the large MVA-rating and inertia of SG_1 compared to the other SGs means that even when SG_1 is the low-cost SG (with 100% active power loading), SG_3 (medium-cost) is the CSG in the LHM cost allocation. This is due to the fact that a machine with smaller inertia requires less energy (and so less time) to advance the rotor angle beyond the stability limit, highlighting the fact that angular stability also depends on the aforementioned non-operational parameters.

The results that follow illustrate how locational aspects and generator sensitivity to active power loading (determined by cost) in the context of displacement of SG by PEC impact stability from the base case presented above.

3.2. Impact of Locational Aspects with Increased Penetration of Power Electronic Converter Interfaced Generation

As displacement of SG by PEC increases, there is a distinct impact on angular stability depending on the location

of the PEC compared to SG. In general terms, the displacement of a SG by PEC in the same area has a beneficial impact on the stability of that SG (reflected by an increase in CCTs for faults where that SG is the first to go unstable), whilst the stability of SGs in a further away area deteriorates (reflected in a decrease in CCTs for faults where that SG is the first to go unstable). It is highlighted that in certain scenarios, this locational improvement/deterioration in the stability boundary can result in a switch in the CFL and CSG.

These reasons for improvements/deteriorations in the stability of SG between displacement cases can be analysed using locational parameters defined in Section 2.5. These include admittance between various network locations (Table 5), the EDR (Table 6), and short circuit capacity (Table 7).

Table 5 Admittance in p.u. from generation source to different network locations in each displacement case

from	SG_2				SG_3				PEC	
to	Bus 2	Bus 5	Bus 6	Bus 8	Bus 3	Bus 5	Bus 6	Bus 8	Bus 2	Bus 3
Base	5.5	3.3	2.8	4.1	4.2	2.4	2.7	3.1	-	-
1	4.5	2.9	2.5	3.5	4.2	2.4	2.7	3.1	16.7	2.3
2	3.3	2.3	2.1	2.7	4.2	2.4	2.7	3.1	33.8	2.5
3	1.8	1.5	1.4	1.6	4.2	2.4	2.7	3.1	50.7	2.6
4	5.5	3.3	2.8	4.1	3.3	2.1	2.3	2.6	2.4	8.8
5	5.5	3.3	2.8	4.1	2.4	1.7	1.8	2.0	2.7	17.5
6	5.5	3.3	2.8	4.1	1.3	1.0	1.1	1.1	2.9	26.2

Table 6 Electrical Distance Ratio (EDR) for SG_2 and SG_3 in each displacement case

Case	SG_2 x_d' / x_{grid}	SG_3 x_d' / x_{grid}
Base	-	-
1	1.30	0.73
2	2.60	0.83
3	5.83	0.87
4	0.39	1.41
5	0.48	3.13
6	0.52	7.50

Table 7 Synchronous short-circuit capacity (MVA) at different network locations for all displacement cases

Case	Bus 2	Bus 3	Bus 5	Bus 6	Bus 8
base	1379.78	1080.44	879.38	837.3	933.26
1	-17%	-1%	-3%	-1%	-5%
2	-35%	-4%	-7%	-4%	-12%
3	-52%	-7%	-13%	-7%	-21%
4	-1%	-15%	-1%	-3%	-4%
5	-3%	-30%	-3%	-6%	-9%
6	-5%	-44%	-6%	-12%	-16%

Three case studies are used to illustrate these locational aspects; Fig. 3, Fig. 4 and Fig. 5 where CCTs at key fault locations for the MLH, MHL and HLM cost allocations are given for each displacement case respectively. The first SG to go unstable for each fault is also represented on the graph by the SG number (1, 2 or 3). Although not explicitly analysed in this section, the analysis that follows holds for all cost allocations, including HML (Fig. 6) which is presented in succeeding sections.

Firstly, the difference in the CFL between the MLH and MHL cost allocations can be analysed (Fig. 3 and Fig. 4). In line with Section 3.1, the low-cost SG is the CSG. For example, in Fig. 3 SG_2 is low-cost and is the CSG with the CFL being at bus 2 in all displacement cases. In Fig. 4, SG_3 is the low-cost SG and is also the CSG with the CFL at bus 3 in all displacement cases. This is the case despite significant variations in CCTs throughout the network between displacement cases. For example, CCT_2 in Fig. 3 (the CFL) varies by up to 80 ms and CCT_3 in Fig. 4 (the CFL) varies by

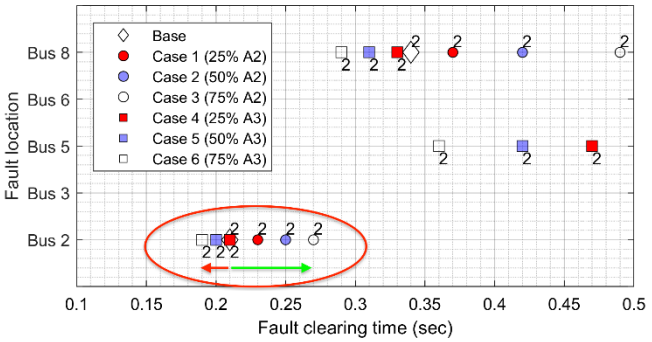

Fig. 3. *MLH cost allocation - CCTs at key fault locations for all displacement cases. CFL at bus 2 in every case.*

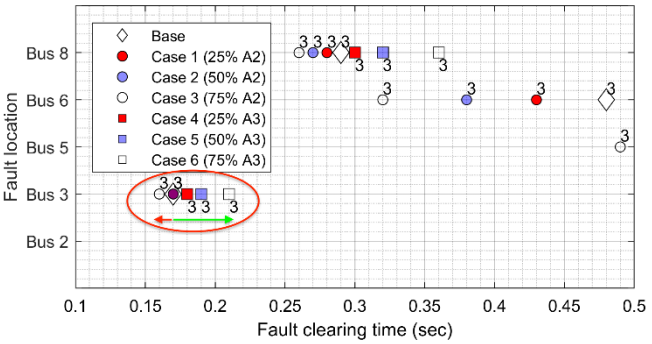

Fig. 4. *MHL cost allocation - CCTs at key fault locations for all displacement cases. CFL at bus 3 in every case.*

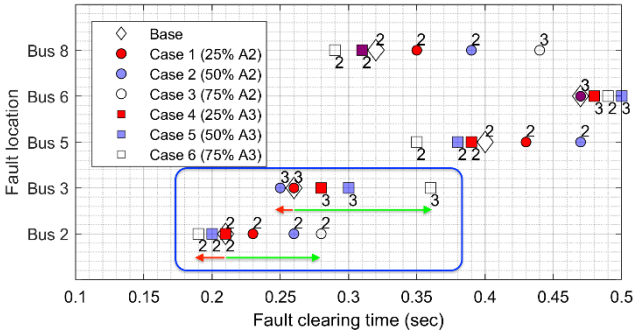

Fig. 5. *HLM cost allocation - CCTs at key fault locations for all displacement cases. Switch in CFL and CSG as a result of locational aspects.*

up to 50 ms. This results in large variations in CCT_{min}, along with variations in CCTs throughout the network in both cases. Whether there is an improvement or deterioration depends on the fault location with respect to the location of displacement – with CCTs improving for faults where the first SG to go unstable is displaced by PEC, and deteriorating for faults where the first SG to go unstable is not displaced (i.e. displacement of an SG by PEC improves the stability of that SG). In Fig. 5 (HLM), the combined effect of an increase in CCT_2 and decrease in CCT_3 results in a switch in CSG and CFL between displacement cases 1 and 2. Additionally, the CSG switches from being the low-cost SG_2 and, to being the medium-cost SG_3 (blue box in Fig. 5). Using the locational parameters defined in Section 2.5, the reasons for both improvements and deteriorations in the stability boundary are analysed in Sections 3.2.1 and 3.2.2 respectively.

3.2.1. Locational Aspects of Angular Stability Enhancement (green arrows): For the cases that there is an improvement in transient stability (green arrows), the locational metrics used (electrical distance and system strength) tend to show a consistent behaviour as described

below. As an SG is displaced, the admittance between this displaced SG and all network locations decreases (due to decrease in the machine rating and consequent increase in x_d' of the machine), causing the fault to be seen electrically further from the generator internal voltage. In addition to this, as displacement increases PEC becomes electrically closer to the network (since an increase in the number of PECs connecting to the network in parallel results in an increase in admittance between PEC and the grid). In cases studied is this paper, this also results in PEC becoming electrically closer to SG. This means that the FRT capabilities of PEC (a rapid reduction in active power output and injection of reactive power during and right after the fault) are able to support local SGs to a greater extent.

Table 5 shows that between displacement case 1 to case 3, the admittance between PEC and bus 2 increases (from 16.7 p.u. to 50.7 p.u.), whilst the admittance between SG_2 and bus 2 decreases (from 4.5 p.u. to 1.8 p.u.). The net result is that SG_2 becomes electrically closer to PEC. Therefore, any improvements to stability brought about by the FRT capabilities of PEC are able to be realised by SG_2 to a greater extent. For example; in Fig. 3 and Fig. 5, an improvement in CCT_2, CCT_5 and CCT_8 is observed between case 1 and 3 (i.e. fault locations where SG_2 is the first SG to go unstable). Similarly, in Fig. 4 (MHL cost allocation) there is a significant improvement in the stability of SG_3 (reflected in an improvement in CCT_3 from 0.17 seconds in the base case through to 0.21 seconds in case 6). Table 5 shows the network admittance between PEC and bus 3 increasing from 8.8 p.u. in case 4 to 26.2 p.u. in case 6.

As displacement increases, the electrical distance between PEC and the SG that is not displaced also decreases. However, the magnitude of the electrical distance between the PEC and SGs that are not displaced is found to be too large for any benefits brought about by the FRT capabilities of PEC to support them (e.g. although the admittance between bus 2 and PEC increases slightly from 2.4 to 2.9 p.u. between case 4 and 6 in Table 5, their overall electrical distance is higher compared to the admittance from PEC to bus 3 (8.8 to 26.2 p.u.)). In cases where there is a large electrical distance between any given SG and PEC, the stability of that SG is found to deteriorate. Reasons for this deterioration in angular stability are discussed in more detail in Section 3.2.2.

Table 6 shows the EDR for SG_2 and SG_3 with respect to PEC across all displacement cases. In cases 1-3, SG_2 gets electrically further from the grid and PEC_2 gets electrically closer to the grid – but the extent to which SG_2 gets further from the grid is smaller than the extent to which PEC gets closer to SG_2 – resulting in the EDR increasing from 1.30 in case 1 to 5.83 in case 3 (Table 6). In cases 1-3 for SG_3, the EDR is below 1, indicating that the distance between SG and PEC is larger. In addition to this, PEC gets electrically closer to SG_3 as between cases 1-3 – resulting in an increase in the EDR. However the increase in the EDR is much smaller than in the previous case, since the grid impedance is larger between PEC_2 and SG_3 compared to PEC_2 and SG_2. Since the EDR represents the proximity of PEC to SG (and therefore the ability of PEC to support SG), a large value (above 1) in Table 6 corresponds to an improvement in stability of that SG and subsequent improvement in CCTs at locations where that SG is the first to go unstable.

Table 7 shows the short-circuit capacity at different locations on the network for each of the displacement scenarios. As SG_2 is displaced (cases 1-3), the short-circuit capacity decreases throughout the network – but most significantly at bus 2 (up to a 52% reduction in short-circuit capacity between the base case and case 3 in Table 7). It would be expected that this significant reduction in short-circuit capacity at bus 2 would be reflected in a reduction in CCT_2. However the opposite is true, with CCT_2 increasing from the base case through to cases 1-3 (Fig. 3 and Fig. 5). Similar trends are observable for displacement of SG_3 (with up to a 44% reduction in short-circuit capacity at bus 3 between the base case and case 6) and an improvement in CCT_3 from the base case and cases 4-6 in Fig. 4. This suggests that the benefits to angular stability brought about by PEC being connected close to SG can overcome a significant reduction in network strength.

In general terms, displacement of a SG by PEC in the same area has been shown to have a beneficial impact on the stability of that SG, since; (a) the electrical distance between the SG and the grid increases (due to the reduction in MVA-rating of the displaced SG), (b) the electrical distance between PEC and the displaced SG decreases, (c) the FRT capabilities of PEC is able to support local SG (through rapid reduction in active power output and injection of reactive power), and (d) as the proportion of displacement increases, the increasing volume of PEC (MW) is increasingly able to support the increasingly smaller local SG (in terms of MVA rating) via the aforementioned FRT capabilities of PEC. This is despite a significant reduction in network strength (coming only from synchronous generation disconnection) in the area of displacement.

3.2.2. Locational Aspects of Angular Stability Deterioration (red arrows): This section examines locational reasons for the deterioration in stability of the SG that is not displaced by PEC (indicated by red arrows in Fig. 3 and Fig. 4 and Fig. 5). In cases where the EDR is small (Table 6 values below 1), a deterioration in the angular stability of the SG is observed.

For example, in Fig. 3 CCT_2 reduces in cases 4-6. Similarly, in Fig. 4, CCT_3 reduces between the base case and case 3. In addition to this, as the volume of PEC connected increases, the electrical distance between PEC and the SG that is not displaced reduces. This is reflected in a slight increase in the EDR as displacement increases (e.g. for SG_2, the EDR increases from 0.39 in case 4 to 0.52 in case 6 (Table 6)). Despite this reduction in electrical distance, the CCTs for faults where that SG is the first to go unstable reduce (e.g. in Fig. 3, CCT_2 reduces from 0.21 s in case 4 to 0.19 s in case 6). It is therefore likely that the large electrical distance between the SG and PEC means that the beneficial impact from the FRT capabilities of PEC are unable to enhance the stability of the distant SG.

An additional reason for the reduction in angular stability, relates to a reduction in network strength (i.e. short-circuit capacity) from the perspective of the SG that is not displaced. Between the base case and case 1-3 (where SG_2 is progressively displaced), there is a reduction in short-circuit capacity throughout the network. Although the largest reduction in short-circuit capacity is observed at bus 2, there is also a reduction (although smaller) in short-circuit capacity at bus 3 – meaning that the network appears weaker from the perspective of SG_3. This is observable in Fig. 4, where the

reduction in short-circuit capacity by 7% at bus 3 between the base case and case 3 (Table 7) contributes towards the deterioration in CCT_3 (along with larger reductions CCT_5, CCT_6 and CCT_8, where larger decreases in short-circuit capacity are observed). Similarly in Fig. 3; CCT_2, CCT_5 and CCT_8 reduce (suggesting a reduction in the stability of SG_2) in cases 4-6 as a result of the reduction in short-circuit capacity is observed at bus 2 (Table 7).

In summary, the stability of the SG that is not displaced deteriorates in these studies, since; (a) the point of connection of PEC is too far away for the benefits of FRT capabilities to be realised by the SG that is not displaced, and (b) the strength of the network (short-circuit capacity) from that SGs perspective slightly reduces. If the SG that is not displaced happens to also be the CSG, then the CCT for the system can reduce since the stability of that SG has been found to deteriorate.

3.3. Impact of Sensitivity to Changes in Active Power Output of Synchronous Generation

Along with the locational aspects previously discussed, the sensitivity of an SG to changes in its active power output has also been found to have a significant impact on the stability boundary. Section 3.3.1 provides a case where an SG has a high sensitivity to changes in active power output between displacement cases. In the case presented, the large variations in active power loading results in significant changes to the stability boundary, such that a new CFL and CSG appear in one case. Section 3.3.2 highlights an additional case where a SG has a high sensitivity to changes in active power output, but there is a limited impact on the stability boundary. Finally, Section 3.3.3 provides a case where SG has low sensitivity to changes in active power output. As a result, the reasons for changes to the stability boundary between displacement cases are found to be purely locational (Section 2.5). The sensitivity of a SG to variations in active power output and subsequent variation in angular stability could occur in real time, as wind speeds fluctuate, and the system operator modifies the generator dispatch.

As SG is displaced by PEC in operational or planning timescales, the dispatch of generation – governed by the OPF solver – will vary. This means that the active power loading of SG could significantly vary in real time (with some SGs being more sensitive to changes in active power output than others) which could impact the angular stability of the network. The extent to which an SG is sensitive to changes in active power output depends on SG size (MVA-rating), volume of PEC (MW), SG cost, demand level (MW), network constraints – all of which are considered in the OPF formulation. More specifically, when generator costs and generator sizes (MVA-rating of each SG) are such that the low-cost SG is at maximum active power output and this high-cost SG is at its minimum; any change in active power required from SGs comes from the medium-cost generator – making it highly sensitive to changes in active power output. This is dependent on demand level and displacement scenario. Changes to overall demand level are not considered in this paper, to highlight the impact on sensitivity of SG active power loading coming only from changes in generator cost and PEC displacement.

Table 8 shows the maximum variation in active power output for each SG between the base case and cases 1-3 (displacement in area 2), and for cases 4-6 (displacement in area 3). The SG with highest sensitivity to changes in active power output (and the extent to which it varies) changes depending on the displacement case and cost allocation.

Table 8 Active power % output variation of SGs for displacement in area 2 and 3 for key cost allocations

Displacement area	SG	MLH	MHL	HML	HLM
2	SG_1	-0.7%	50.8%	0.0%	-0.2%
	SG_2	0.0%	0.0%	57.0%	0.0%
	SG_3	0.0%	0.0%	0.0%	-0.7%
3	SG_1	28.5%	-4.1%	0.0%	0.5%
	SG_2	0.0%	0.0%	-4.6%	0.0%
	SG_3	0.0%	0.1%	0.1%	23.3%

Table 9 CCT maximum % deviation from the base case at busbars near SG terminals

	MLH	MHL	HML	HLM
bus 1	-49.1%	-66.7%	-21.9%	-22.9%
bus 2	-28.6%	28.6%	151.9%	33.3%
bus 3	-7.0%	23.5%	17.6%	38.5%

Table 9 shows the maximum variation in CCT_1, CCT_2 and CCT_3 from the base case (expressed as a percentage difference from the base case CCTs given in Table 4) at busbars near SG terminals for all displacement cases and key cost allocations. A correlation between a large variation in active power output of a SG and a large variation in CCTs (Table 8) at the busbar local to that generator can be observed. It should be noted however, that this is not the only factor that will influence angular stability as discussed previously (Section 3.1), since all factors (such as generator cost, PEC dynamics, locational aspects and sensitivity to changes in active power) combine to produce an overall result. Because of this, in specific network; a high sensitivity of SG_1 to changes in active power output is not as critical, since either SG_2 or SG_3 are always the CSG. Therefore cases where SG_2 or SG_3 have a high sensitivity to changes in active power output will have a greater impact on angular stability. This is evident in the HML cost allocation where SG_2 varies by up to 57.0% (Table 8) and CCT_2 varies by 151.9% (Table 9).

3.3.1. Significant impact on network stability of SG having high sensitivity to changes in active power output: In the example presented, the combined effect of SG_2 having a high sensitivity to changes in active power loading, locational aspects (discussed in Section 3.2), non-operational parameters and the dynamics of Type IV wind result in the CFL and CSG changing. Being the low-cost generator, SG_3 is the CSG in the base case for this cost allocation. However, the high sensitivity of SG_2 (originally not the CSG) to changes in active power output between different displacement scenarios results in significant changes to the stability boundary. In case 6, CCT_2 and CCT_3 become equal (for the resolution used), meaning that both bus 2 and 3 are CFLs and SG_2 and SG_3 CSGs, respectively. This change in CFL and CSG can be largely attributed to an increase in SG_2 active power loading between case 4 and 6 which results in a reduction in CCT_2. At the same time, an enhancement in the stability of SG_3 (brought about through the locational aspects outlined in detail previously), results in an increase in CCT_3) such that there are two CFLs and CSGs in case 6 (highlighted by a red box in Fig. 6).

Fig. 7 shows the active power loading of each SG in the HML case for each displacement case. The minimum and

maximum active power limits (in MW) of each SG are shown by black upper and lower bounds and the MW dispatch given block colour. The active power loading (in %) of each SG is shown by a coloured dashed line. Crucially, it can be seen that the active power output of SG_2 (the medium-cost SG) varies significantly between displacement cases (up to 59%), indicating a high sensitivity to changes in active power output compared to the other SGs on the network (which operate at maximum (100%) or minimum (35%) active power output depending on the generator cost).

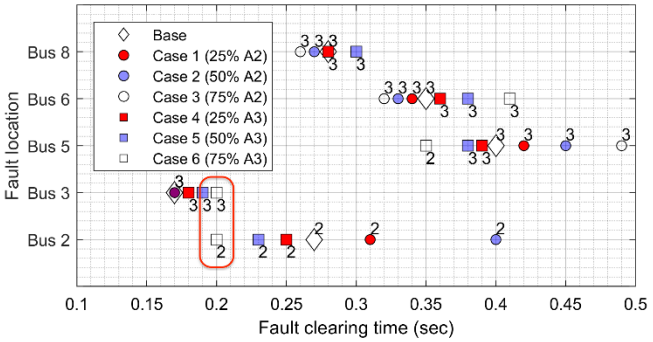

Fig. 6. *HML cost allocation - CCTs at key fault locations for all displacement cases. Additional CFL and CSG in case 6.*

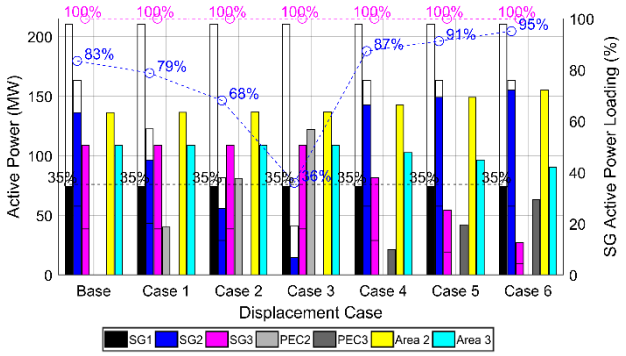

Fig. 7. *HML cost allocation – active power dispatch and loading of SGs. High sensitivity to changes in active power loading of SG_2.*

Between the base case and cases 1-3; since the volume of PEC_2 connecting in area 2 is greater than the reduction in the size of SG_2, and the high-cost SG (SG_1) is at its minimum stable export, there is a reduction in the active power loading of SG_2 (despite its reducing MVA-rating). Since SG_3 is low-cost, it is dispatched at maximum stable export. Between the base case and cases 4-6; the volume of PEC connecting is less than the reduction in size of SG_3, resulting in a reduction in the net export from area 3 (since the MW increase from PEC is not proportional to reduction in the maximum stable MW export of SG in displacement cases (Table 2)). The power deficit is taken up by SG_2, once again resulting in a large variation in its active power output compared to other SGs.

The large variation in SG_2 active power loading is reflected in the significant variation in CCTs at the generator terminal busbar (bus 2 in Fig. 6). There appears to be a strong correlation between a reduction/increase in SG_2 loading and an improvement/deterioration in CCT_2. This suggests that a high sensitivity of an SG to changes in active power loading can significantly influence the angular stability of the network. More specifically, between the base case and displacement case 3, the active power loading of SG_2 reduces by 47%. This reduction in active power loading is reflected in a significant improvement in CCT_2 (from 270 to 680 ms (not visible on scale used in Fig. 6)). Similarly, the active power loading of SG_2 increases by 12% between the base case and case 6, resulting in CCT_2 reducing by 70 ms. The trend in CCT_5 between displacement cases mirrors that of CCT_2 despite SG_3 being the CSG in all cases other than case 6 where the CSG switches to SG_2. This highlights the impact that the loading of SG_2 is having on the dynamic response for faults throughout the network.

There is no change to the active power loading of SG_3 from case 1-3 (Fig. 7), and no change in CCT_3 (Fig. 6) since it is the low cost SG and therefore dispatched at maximum stable MW export. Between cases 4-6 there is an improvement in CCT_3, despite there being no change to the active power loading of SG_3. This disparity between SG_3 loading and CCT_3 indicates that the reason for changes in angular stability are likely to be because of other factors (such as locational aspects, discussed in Section 3.2) and not as strongly related to active power loading.

3.3.2. Minimal impact on network stability of SG having a high sensitivity to changes in active power output: A SG can have a high sensitivity to changes in active power output, but the impact on the stability boundary may be minimal. For example in the MHL cost allocation SG_1 has a high sensitivity to changes in active power output (Fig. 8), but there is a limited impact on the CSG (SG_3 in Fig. 4), CCT and CFL (bus 3 in Fig. 4). This is because in this case the high active power loading and small size (inertia/MVA rating) of SG_3 results in it being very unstable compared to SG_1, meaning that the SG_3 plays the main role in determining overall network stability.

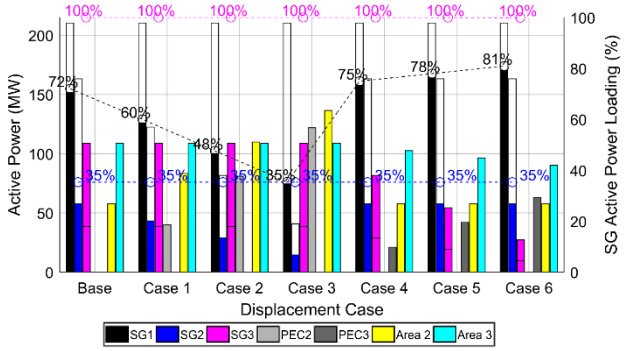

Fig. 8. *MHL cost allocation – active power dispatch and loading of SGs. SG_1 high sensitivity to changes in active power loading.*

3.3.3. Low sensitivity to changes in active power output: In contrast to the high sensitivity cases above, the HLM cost allocation reveals SGs as having low sensitivity to changes in active power output, as shown in Fig. 9. Between cases 1-3, there is no change to the total active power coming from each area, as the active power increase from PEC_2 is countered by the reduction in size of SG_2 (which operates at maximum output since it is the cheapest SG). In cases 4-6, as PEC_3 increases output, there is a slight reduction in active power loading of SG_1 since it is the high cost machine. Since SG_1 is already operating close to its minimum stable output, the active power loading of SG_3 is also reduced by the OPF solver. This is because the incremental costs of SG_1 and SG_3 are very similar in this cost allocation (Table 3). Compared to the high sensitivity case presented in Section 3.3.1, generators in this example have a relatively low sensitivity to changes in

active power output. Despite this, there is still a significant variation in CCTs throughout the network between the different displacement cases (Fig. 5), due to aspects discussed in Section 3.2.

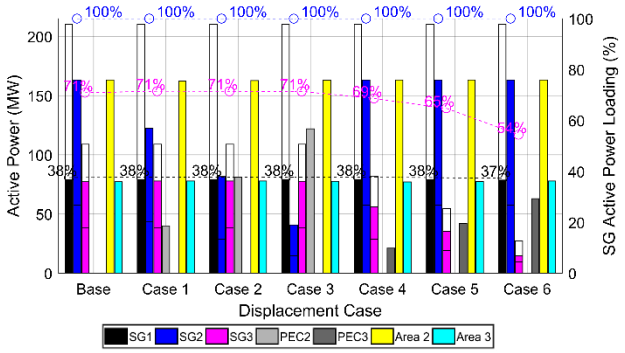

Fig. 9. *HLM cost allocation – active power dispatch and loading of SGs. Small variations in active power loading.*

In general terms, when the difference between generator incremental costs is substantial – such that the high-cost SG is dispatched at its minimum stable export, the low-cost SG at its maximum stable export – any changes in PEC output or demand level (changes to demand are not studied in this paper) are taken up by the medium-cost SG. For example, incremental costs in the HML cost allocation for SG_1, SG_2 and SG_3 are 1.47, 0.95 and 0.14 £/MW respectively (Table 3). This results in a high sensitivity to changes in active power export of SG_2 in Fig. 7 (the medium-cost SG). However, when generator incremental costs are closer, any such changes to PEC output or demand are taken up by multiple generators (e.g. in the HLM cost allocation (Fig 9), active power loading of both SG_1 and SG_3 varies, since their incremental costs are similar (1.47 and 1.42 £/MW Table 3)).

4. Discussion

Results presented in this paper highlight that as the generation mix varies, the 'most critical' fault on a network could change in terms of CCT_{min}, CFL and CSG. These changes to the angular stability boundary may be a result of both long-term planning decisions to decommission specific types of power plants and operational decisions driven by cost, the variability of wind generation and the dynamic behaviour of PEC. Therefore, planning and operational recommendations can be extracted from results presented in this paper.

In planning timescales, connecting windfarms close to generators could lead to improvements in the transient stability of that group of generators, whilst the stability of more distant generators may deteriorate. Therefore, connecting windfarms closer to the critical generators on the network may lead to an overall improvement in the angular stability boundary. In operational timescales the uncertain nature of wind may result in changes to generator dispatch. As a result of changes to the dispatch and the dynamics of PEC; the CFL and CSG will vary in operational time, thus changing the understanding of typical lists of critical contingencies. This paper has demonstrated that there is a trade-off between the most cost effective dispatch and angular stability. Dispatch could be altered – through new ancillary services – to provide a more stable (but also more costly) dispatch.

5. Conclusion

This paper highlights changes to the stability boundary caused by displacement of synchronous generation (SG) by power electronic converter interfaced generation (PEC) as a result of operational and/or planning decisions. A framework to identify and investigate such changes is presented in this paper. Using RMS models and time domain simulations, changes to the stability boundary have been attributed to two main factors; (a) locational aspects and (b) generator cost aspects. Locational aspects are investigated through analysing the electrical distance between key network locations via the network admittance matrix and the electrical distance ratio (EDR - defined in this paper). Generator cost aspects are analysed through marginal costs and the absolute difference between different costs and the subsequent impact on generator dispatch.

Results presented in this paper consistently highlight that – in the test network used – the displacement of SG by PEC in a given area improves the CCTs in that area, whilst reducing the CCTs in other generating areas. This can either lead to an improvement or deterioration in CCT_{min}, depending on the cost of the generator being displaced, and may result in a switch in both CFL and CSG. Locational aspects defined in this paper are able explain these trends; with improvements to the stability boundary being explained through the beneficial impact of FRT capability from PEC being able to support nearby SG (quantified through the EDR). Conversely deteriorations in stability are attributed to a reduction in short circuit capacity.

Moreover, the significance of the sensitivity of the CSG to changes in its active power output (dictated by generator marginal costs and the OPF solution) has been demonstrated by highlighting changes in CFL and CSG of the network. It is demonstrated that when there is a significant difference in SG marginal costs, displacement of SG by PEC can result in a high sensitivity of changes to the active power output of SGs which can significantly impact angular stability. This is because any changes in active power loading are taken up by a single SG. Conversely, there is a limited impact on the stability boundary when generator costs are closer since SGs share any changes in active power loading between them.

Overall, results highlight the importance of generator cost, along with spatial and temporal aspects in changes to system dynamics that must be considered in both planning and operational timescales to ensure secure operation of the network. It has been demonstrated in a test network that; (a) connecting windfarms close to generators that frequently run at full output could lead to improvements in angular stability for local generators whilst more distant machines stability may deteriorate, and (b) the uncertain nature of wind can vary the loading of conventional generation such that the CFL and CSG could change.

6. Acknowledgments

This work was funded by EPSRC CDT in Future Power Networks and Smart Grids at the University of Strathclyde and Imperial College London. ID: EP/L015471/1. All results can be fully reproduced using the methods and data described in this paper and provided references.

7. References

[1] Tielens P, Hertem D Van. The relevance of inertia in power systems. Renewable and Sustainable Energy Reviews, 2016;55(1):999-1009. https://doi.org/10.1016/j.rser.2015.11.016

[2] European Comission, Communication from the Commission to the European Parliament and the Council: Achieving the 10% electricity interconnection target, 2015. Available: https://bit.ly/2LmyOuA, Accessed on: 04/07/2019.

[3] Kundur P et al., Definition and classification of power system stability IEEE/PECRE joint task force on stability terms and definitions, IEEE Transactions on Power Systems, 2004;19(3):1387-1401. https://doi.org/10.1109/TPWRS.2004.825981

[4] P. Kundur, N. J. Balu, and M. G. Lauby. Power system stability and control. McGraw-Hill New York; 1994. https://bit.ly/2xctfa1

[5] Milano F, Dörfler F, Hug F, Hill DJ and Verbič G. Foundations and challenges of low-inertia systems. 20th Power Systems Computation Conference (PSCC), 2018. https://doi.org/10.23919/PSCC.2018.8450880

[6] Edrah M, Lo KL, and Anaya-Lara O, Impacts of high penetration of DFIG wind turbines on rotor angle stability of power systems, IEEE Transactions on Sustainable Energy 2015;6(3):759-766. https://doi.org/10.1109/TSTE.2015.2412176

[7] National Grid, GC0062: Fault ride through, 2015. Available: https://ngrid.com/2LUETvg, Accessed on: 04/07/2019.

[8] Gautam D, Vittal V and Harbour T. Impact of increased penetration of DFIG-based wind turbine generators on transient and small signal stability of power systems. IEEE Transactions on Power Systems 2009;24(3):1426-1434. https://doi.org/10.1109/TPWRS.2009.2021234

[9] Papadopoulos PN and Milanović JV. Probabilistic framework for transient stability assessment of power systems with high penetration of renewable generation. IEEE Transactions on Power Systems 2017;32(4):3078-3088. https://doi.org/10.1109/TPWRS.2016.2630799

[10] Slootweg JG and Kling WL. Impacts of distributed generation on power system transient stability. IEEE Power Engineering Society Summer Meeting 2002;2:862-867. https://doi.org/10.1109/PESS.2002.1043465

[11] Qi B, Hasan KN and Milanović JV, Identification of critical parameters affecting voltage and angular stability considering load-renewable generation correlations, IEEE Transactions on Power Systems, 2019;34(4): 2859-2869. https://doi.org/10.1109/TPWRS.2019.2891840

[12] Meegahapola L and Littler T. Characterisation of large disturbance rotor angle and voltage stability in interconnected power networks with distributed wind generation. IET Renewable Power Generation 2015;9(3):272-283. https://doi.org/10.1049/iet-rpg.2013.0406

[13] Mitra A and Chatterjee D, A sensitivity based approach to assess the impacts of integration of variable speed wind farms on the transient stability of power systems, Renewable Energy 2013;60:662-671. https://doi.org/10.1016/j.renene.2013.06.002

[14] Ma M, Jie W, Wang Z and Khan MW. Global geometric structure of the transient stability regions of power systems. IEEE Transactions on Power Systems (Early Access). https://doi.org/10.1109/TPWRS.2019.2919442

[15] Chen X, Du W and Wang HF. Power system angular stability as affected by the reduced inertia due to wind displacing synchronous generators. 2nd International Conference on Power and Renewable Energy (ICPRE), 2017. https://doi.org/10.1109/ICPRE.2017.8390567

[16] Munkhchuluun E, Meegahapola L and Vahidnia A. Impact on rotor angle stability with high solar-PV generation in power networks. 7th IEEE PES Innovative Smart Grid Technologies Conference Europe (ISGT-Europe), 2017. https://doi.org/10.1109/ISGTEurope.2017.8260229

[17] Ortega Á and Milano F. Stochastic transient stability analysis of transmission systems with inclusion of energy storage devices. IEEE Transactions on Power Systems 2018;33(1):1077-1079. https://doi.org/10.1109/TPWRS.2017.2742400

[18] Johnstone K, Bell K, & Booth C. The impact of post-fault active power recovery ramp rates of wind turbines on transient stability in Great Britain. European Wind Energy Association (EWEA) Annual Event, 2015. https://bit.ly/2YzqDlX

[19] Zhang Y, Ding M, Han P, Sun H, Yang W and Chen Z. Analysis of the interactive influence of the sctive power recovery rates of DFIG and UHVDC on the rotor angle stability of the sending-end system. IEEE Access (Early Access). https://doi.org/10.1109/ACCESS.2019.2923341

[20] Bakhtvar M, Vittal E, Zheng K and Keane A. Synchronizing torque impacts on rotor speed in power systems. IEEE Transactions on Power Systems 2017;32(3):1927-1935. https://doi.org/10.1109/TPWRS.2016.2600478

[21] Xu Y, Xie X, Dong Z. Y., Hill D. J., and Zhang R. Risk-averse multi-objective generation dispatch considering transient stability under load model uncertainty. IET Generation, Transmission & Distribution 2016;10(11):2785-2791. http://doi.org/10.1049/iet-gtd.2015.1502

[22] Calle I. A, Ledesma P, and Castronuovo E. D. Advanced application of transient stability constrained-optimal power flow to a transmission system including an HVDC-LCC link. IET Generation, Transmission & Distribution 2015;9(13):1765-1772. https://doi.org/10.1049/iet-gtd.2015.0215

[23] Anderson P, Fouad A, and Happ H. Power system control and stability. IEEE Transactions on Systems, Man, and Cybernetics 1979; 9(2):103-103. https://doi.org/10.1109/TSMC.1979.4310158

[24] Sorensen P, Andresen B, Fortmann J, and Pourbeik P. Modular structure of wind turbine models in IEC 61400-27-1. IEEE Power and Energy Society General Meeting (PES) 2013:1-5. https://doi.org/10.1109/PESMG.2013.6672279

[25] Vittal E, O'Malley M, and Keane A. Rotor angle stability with high penetrations of wind generation. IEEE Transactions on Power Systems 2012;27(1):353-362. https://doi.org/10.1109/TPWRS.2011.2161097

[26] Dommel H and Tinney W. Optimal power flow solutions. IEEE Transactions on Power Apparatus and Systems 1968;10:1866-1876. https://bit.ly/2XlNy46

[27] UK Government. BEIS electricity generation costs, 2016. Available: https://bit.ly/2Fd5bFk, Accessed on: 04/07/2019.

[28] International Electrotechnical Commission. Short-circuit currents in three-phase AC systems standard (IEC 60909-0). Available: https://bit.ly/30dA1se. Accessed on: 04/07/2019.